



# Flexural behavior of corroded one-way slabs strengthened with CFRP in two different techniques

Ruqaya K Ibrahim<sup>1</sup> · Assim M Lateef<sup>1</sup>

Received: 7 June 2024 / Accepted: 22 July 2024 / Published online: 20 August 2024  
© Springer Nature Switzerland AG 2024

## Abstract

The experimental investigation conducted in this paper investigates the flexural behavior of corrosion-damaged reinforced concrete (RC) slabs reinforced with carbon fiber-reinforced polymer (CFRP) using two different techniques, namely NSM with CFRP ropes and CFRP strips. The steel reinforcing bars of the examined slabs underwent corrosion induction using an accelerated corrosion approach. This study included three groups of corroded slabs (weak, moderate, and sever corrosion), two models in each group that were strengthened using CFRP in two different ways, with a reference model in each group. Weight loss percentages for each corrosion level is were 11%, 26%, and 40%, respectively. The result showed that not only the yielding and ultimate capacities of the reinforced slabs were recovered, but they also outperformed those of the virgin control slab. Slab strengthened with CFRP strips showed an increased in yielding strength from 15 to 65%, 20–53%, and 38–58% for 10,17, and 24 days, respectively. Also, for NSM, an increase in the yield strength from 15 to 38% and from 20 to 23% was recorded. While, for the 40% corrosion a clear reduction in the yield strength was recorded due to losing a third of the depth of the section due to the effect of steel corrosion as well as losing some of the steel cross-sectional area. Results show that increasing corrosion levels from 11 to 42%, reduce the strengthening of the load capacity of the slab to the applied loads from 38 to 15%. It is worth mentioning that the examined reinforced slabs were failed due to both yielding in the steel reinforcing bars as well as compression crushing of the concrete.

**Keywords** Slab strengthening · Corroded slabs · CFRP strengthening · NSM · Fiber-reinforced polymer

## Introduction

The usage of concrete buildings is the most common in architectural and civil engineering. It is well known that corrosion of the reinforcing rebars is one of the main issues with RC constructions' endurance in harsh environments [1]. Many structures had to be strengthened or restored since the corrosion of the reinforcing steel had made them less safe and able to support loads. The corrosion of steel bars in concrete has a substantial impact on the strength and stiffness of structures, particularly in terms of their structural performance [2]. Corrosion of reinforcing rebars leads to a decrease in their cross-sectional areas and a decline

in their strength, ductility, and other mechanical qualities [3]. Corrosion products have the ability to create expansion pressures that can change the stress conditions in concrete, leading to the formation of fractures and causing damage to slabs. Furthermore, the corrosion of reinforcing rebars can also reduce the bonding strength between the corroded rebars and the adjacent concrete. Specifically, the creation of fractures in concrete diminishes its capacity to confine reinforcing bars. Moreover, the corrosion of reinforcing rebars might diminish the mechanical cohesion between the distorted ribs of the rebars and the concrete. The parameters described above can greatly influence the flexural capacity and failure mechanism of reinforced concrete slabs that have experienced corrosion [4–6].

Repairing or strengthening RC structures that have corroded reinforcing rebars is essential to restore the structural bearing capability. Common techniques for reinforcing reinforced concrete (RC) elements include section enlargement, steel bonding, the external steel-clad approach, and carbon fiber reinforced polymer (CFRP) strengthening. FRP

✉ Ruqaya K Ibrahim  
RK230007en@st.tu.edu.iq

✉ Assim M Lateef  
assaim77@tu.edu.iq

<sup>1</sup> Tikrit University, Alam, Iraq

composites have effectively enhanced the strength and flexibility of reinforced concrete elements that have sustained significant damage in various situations, including earthquakes, fire incidents, and others [7].

Since the beginning of the twenty-first century, CFRPs have become increasingly popular in the rehabilitation of corroded steel buildings. Many scientists throughout the world have researched numerous parameters that influence the flexural performance of CFRP-strengthened corroded RC beams. Factors affecting reinforcing rebars include corrosion [15], mechanical behavior [16], quantity of CFRP sheets [17], anchoring [18], strengthening schemes [15], bond behavior of corroded rebars at the concrete interface [16], initial load, and damaged concrete cover [19–23].

Pilot research conducted by Soudki and Sherwood [10] investigated the prospect of using CFRP reinforcement to bend corroded RC beams. The study examined ten beams with varying corrosion levels of 5%, 10%, and 15%, including six with CFRP sheets, to demonstrate their ability to recover specimen integrity and capacity. The investigation found that CFRP sheets can improve the strength and capacity of corrosion-damaged concrete beams. Kashi et al. [24] studied the impact of maritime environmental conditions on the endurance of corroded RC columns reinforced with FRP using three retrofitting methods. After nine thousand hours of maritime exposure, the ultimate strength of the retrofitted columns made of one layer of CFRP sheet and GFRP in retrofit technique one dropped by 19.7% and 27.4%, respectively. In retrofit method two, the ultimate strength of columns covered in one layer of CFRP and GFRP decreased by 18.3% and 25%, respectively. In retrofit method three, the ultimate strength of reinforced columns with one or two GFRP layers increased by 8.8% and 2.2%, respectively, after 9000 h of maritime exposure.

Researchers evaluated the structural performance of aramid fiber reinforced polymer (AFRP) -strengthened corroded RC beams [25, 26]. Gotame, M. et al. [27] studied non-linear finite element studies used to determine the flexural behavior of corrosion-damaged RC beams reinforced with externally bonded FRP, reached that enough

flexural strengthening was given by an inclined U-jacket at the extremities of the CFRP plate and a CFRP plate at the beam soffit. Consequently, the load-bearing capability for the investigated beam geometry and corrosion damages was not further increased by intermediate U-jackets. Zheng et al. [28] investigated the shear behavior of reinforced concrete (RC) beams with corrosion-damaged stirrups enhanced with FRP and an ECC matrix, the shear bearing capacity of the beams with corrosion-damaged stirrups dramatically increased when they were rebuilt using this procedure, according to the testing data. After FRP retrofitting, Van Cao et al. [8] investigated the behavior of reinforced concrete slabs subjected to fire. According to the research results, fire considerably decreased the stiffness by around 30% but only slightly decreased the yield and final strengths. For fire-exposed slabs, retrofits using 1/2 and 1 FRP layer raised the ultimate strength by 46% and 65% and the yield strength by 30% and 45%, respectively. Because of carbon fiber-reinforced polymer (CFRP) is lightweight, easy to manufacture, and durable, it is a useful method for reinforcing corroded reinforced concrete slabs [9].

Because of its superior strain-hardening behavior, the engineered cementitious composite (ECC) enhances the specimen's deformation properties and energy absorption while the embedded FRP grid efficiently shares the shear force supported by the stirrups. Yang J. et al. [29] tested the effectiveness of employing externally bonded FRP laminates and U-jackets to reinforce beams with corroded reinforcing rebars, without fixing the degraded concrete cover. The shear span-to-depth ratio of an RC beam reinforced with EBR-FRP composites can impact its behavior and define its failure mode [30]. Chen et al. [31] presented ultra-high-performance concrete (UHPC) and fiber-reinforced polymer (FRP) composites for the shear strengthening of corroded reinforced concrete beams.

Based on the best knowledge of the researches, no studies have been conducted related to the flexural behavior of RC slabs that exposed to corrosion and were reinforced using CFRP. The study tested ten RC slabs with accelerated corrosion of longitudinal reinforcing rebars at different levels. Following the corrosion, six of the slabs were reinforced with CFRP using two techniques (sheets and NSM) on the tension side to restore the strength loss caused by the corrosion.

## Experimental study

### Casting and curing of concrete slabs

This study used river sand in the presented mixture. Table (1) illustrates the performance of cement, fine aggregate,

**Table 1** Description of materials

Material	Description
Cement	Type I ordinary Portland cement is consistent with Iraqi specification No.5/1984
Coarse Aggregate	The concrete mix design satisfies the IQS No.45 standards by using river gravel with a maximum size of 12.5 mm and a rounded partial form
Fine Aggregate	The necessary concrete mix design is made from river sand with a maximum size of (4.75) mm and a fineness modulus (F.M = 2.62) that satisfies IQS No.45 specifications
Water	Pristine tap water (used for mixing and curing)
Steel Bar	Deformed steel bar with a diameter of 6 mm

and coarse aggregate. The water-cement ratio of the concrete mixture was 0.45 for all examples, and the masses of cement, water, coarse aggregate, and sand per cubic meter of concrete were 350 kg, 160 kg, 1040 kg, and 850 kg. The cubic concrete compressive strength was 35 MPa. The longitudinal reinforcing rebars were deformed and had a yield strength of 500 MPa. The CFRP composites were made consisting of dry fiber sheets and epoxy resin, and the supplier of carbon fibers and resin provided the mechanical property measurements presented in Table (2). The standard thickness of the composite CFRP sheet was 0.11 mm, 50 mm in width for CFRP strips, and 6 mm in diameter for NSM.

Figure (1) depicts a cross-section of the test specimen, displaying structural features. The test specimens were reinforced concrete slabs that were 1100 mm long by 400 mm wide, with a depth of 70 mm and an effective depth of 60 mm. Tensile reinforcing rebars were constructed from deformed steel with a diameter of 6 mm. The specimen’s construction was meant to cause flexural failure.

**Designed corrosion level and strengthening method**

Table (3) shows the planned corrosion level of the reinforcing rebars as well as the experimental strengthening method. All specimens, save the control slab (S0), were subjected to accelerated corrosion. The direct current (DC) power supply utilized in the accelerated corrosion was made by Shanghai Wenkai Power Supply Equipment Ltd. in Shanghai, China. The research defined corrosion as the bulk loss of reinforcing rebars. Three distinct corrosion levels for longitudinal

**Table 2** Mechanical properties of dry carbon fibers and resin

Material	Tensile strength (MPa)	Tensile modulus (MPa)	Ultimate elongation (%)
Dry Carbon Fibers	3060	2.1 × 10 <sup>5</sup>	1.6
Epoxy Resin	35.5	2040.6	2.1

**Table 3** Test matrix

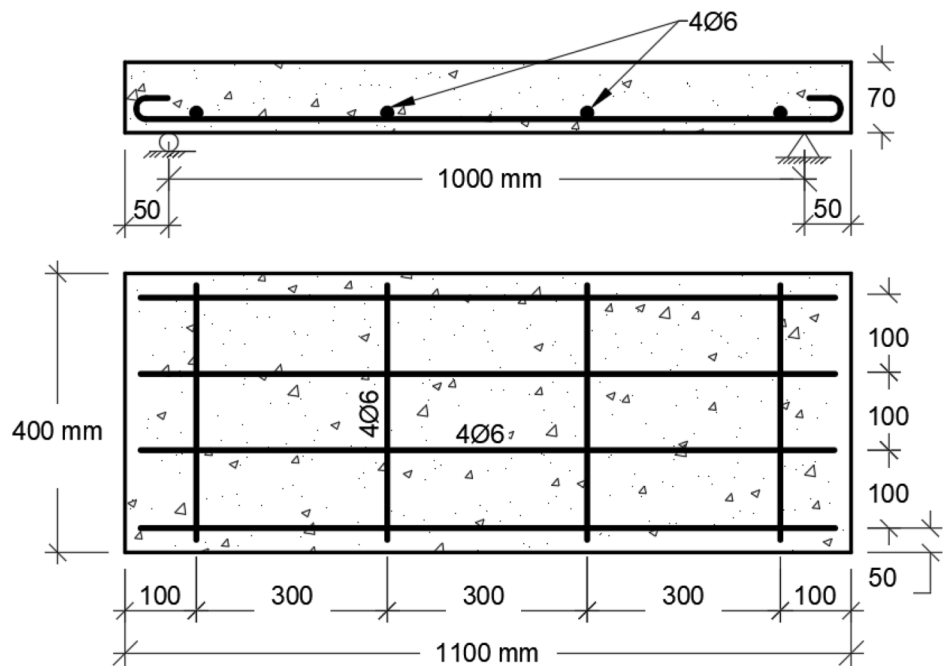
Specimen Number	Designed Corrosion Level (%)	Strengthening Method
S0	0	Main Reference
S1-1	11	Corroded Reference (1)
S1-2	11	CFRP Strips
S1-3	11	NSM
S2-1	26	Corroded Reference (2)
S2-2	26	CFRP Strips
S2-3	26	NSM
S3-1	42	Corroded Reference (3)
S3-2	42	CFRP Strips
S3-3	42	NSM

reinforcing rebars were devised, and all specimens were reinforced with CFRP.

**Accelerated galvanization corrosion mechanism**

To simulate corrosion damage in test specimens, a direct current (DC) power supply from Shanghai Wenkai Power Supply Equipment Ltd. in Shanghai, China was used. After curing the test specimens, they were placed in a sealed tank with a 5% NaCl solution. The liquid level was above the slab surface. The anode consisted of longitudinal reinforcing

**Fig. 1** Tested specimen details



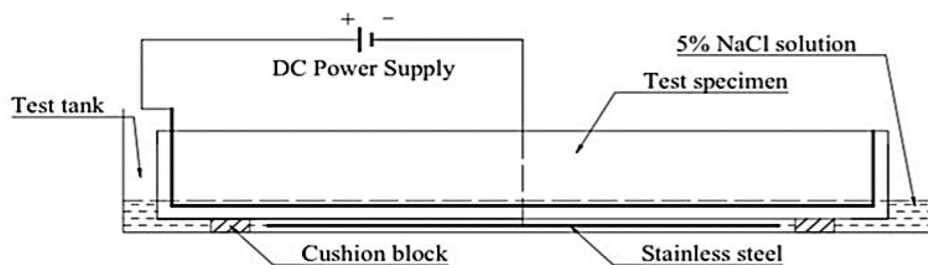
rebars connected to the positive terminal of an external power supply, while the cathode was a stainless-steel rod connected to the negative terminal.

Figure (2) shows the arrangement used for the accelerated corrosion process. A direct current (DC) power supply from Shanghai Wenkai Power Supply Equipment Ltd. in Shanghai, China, with a current density of  $1 \text{ mA/cm}^2$  was used for stability. Faraday's law states that the duration and quantity of current running through reinforcing rebars determines their corrosion levels. Corrosion impairment lasted from 20 h (S1-3) to 576 h (S3-3), resulting in modest to severe damage. Figure (3) depicts slab specimens following the corrosion of the reinforcing rebar.

### Strengthening methods

All test specimens were reinforced using CFRP (three with strips, three with NSM) and compared to the references.

**Fig. 2** Accelerated Corrosion Setup; a) schematic of setup, and b) close up view



(a)



(b)

Figure (4) depicts the configuration of the CFRP reinforcement. One layer of four CFRP sheets of 50 mm width was bonded to the tension face of the slab with a length of 1100 mm, and four CFRP robs for NSM with a diameter of 6 mm and a length of 1100 mm.

The surface of the concrete zone to be bonded with CFRP was polished with a grinding machine. After the surface was washed and cleaned, the CFRP sheets and robs were glued to the slab specimens using epoxy resin. Figure (5) depicts the slab specimen during repair with the FRP.

### 2.5 Test setup and instrument

The specimens required to be cured for seven days after strengthening. We used three electrical dial gauges to measure the strain in the concrete at the slab's midspan. The test setup's configuration is shown in Fig. (6 and 7). After that, two-point loading tests were performed on each slab until it



**Fig. 3** The Investigated RC Slabs Bottom After Corrosion; **a)** Weak Corrosion, **b)** Moderate Corrosion, and **c)** Severe Corrosion

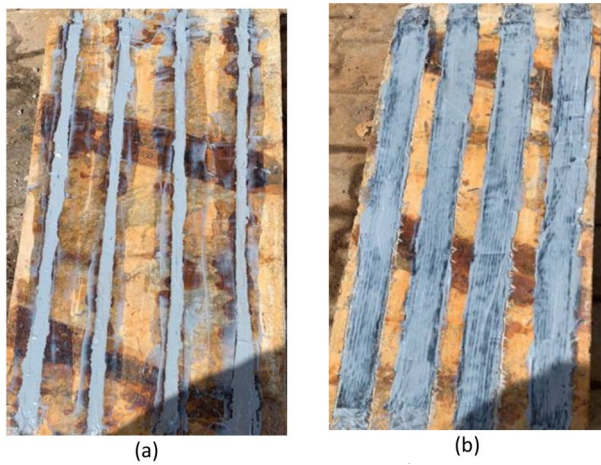
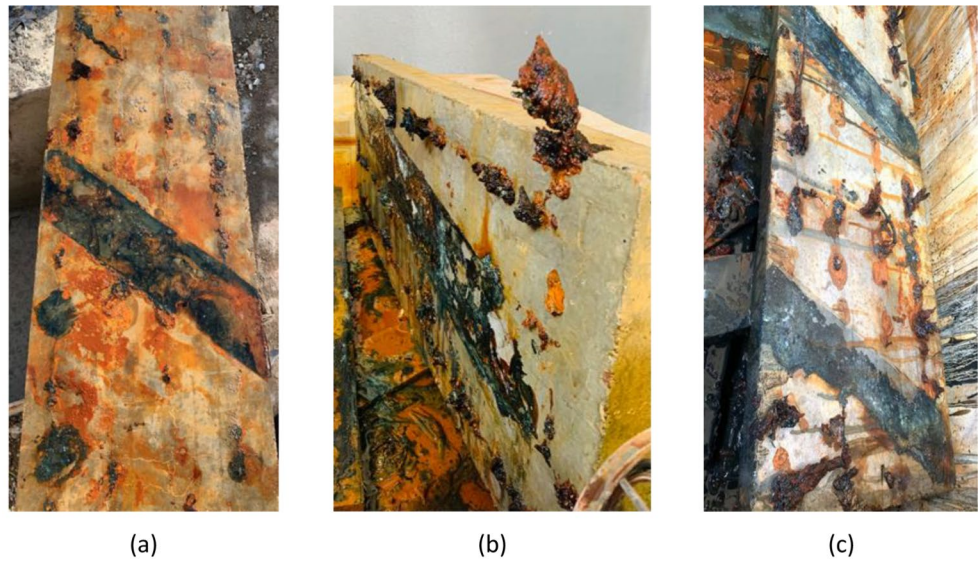


**Fig. 4** Strengthening Methods; **a)** NSM, and **b)** CFRP strips

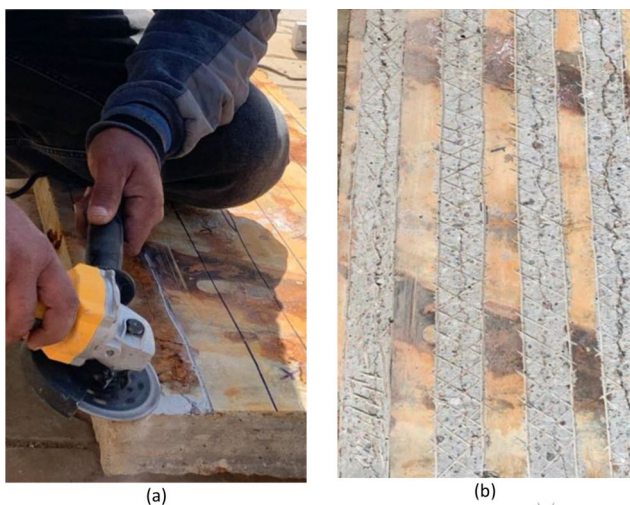


**Fig. 5** **a)** Cleaning the slabs, and **b)** Scratch Shape

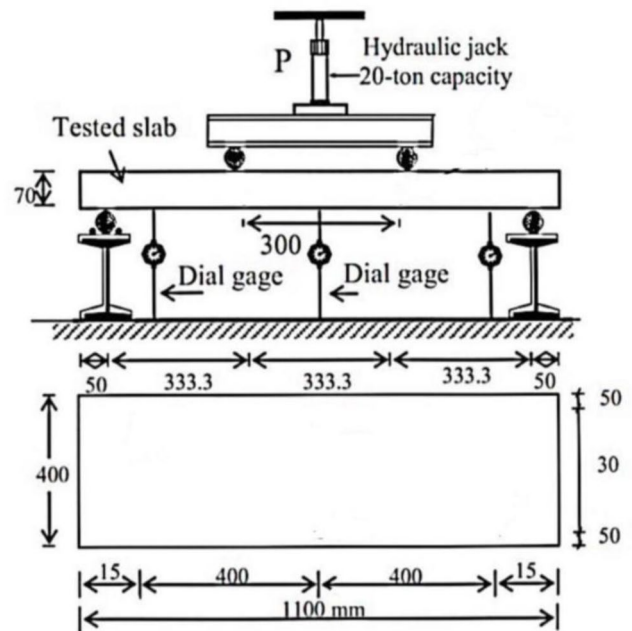


**Fig. 6** Test Setup

failed. The loading points were spaced 333.33 mm apart. Up to failure, the loading was measured via a hydraulic jack and two 20-ton pressure transducers. Installing linear variable displacement transducers (LVDTs) with a 100 mm range capacity (Donghua Testing Ltd., Taizhou, China) allowed for the monitoring of the displacement of the slab at the midspan.



Fig. 7 Slab Test

## Results and discussion

### Corrosion damage and inspection

Following the fast degradation of the longitudinal steel reinforcement, corrosion-related fractures were mapped and reported. The observed fracture patterns were consistent across all corroded specimens. Because corrosion happened at random, the cracks along the longitudinal steel bars were not evenly distributed. After the slab specimens failed to load, three steel coupons were extracted from the corroded longitudinal reinforcing rebars. After removing the rust using diluted hydrochloric acid, the length and weight of the reinforcing rebars were measured. After comparing their weight loss per unit length to that of uncorroded coupons, the observed corrosion degree was determined. Table (4) shows the tension reinforcing rebars before and after corrosion at each corrosion level.

### Carrying load capacity

#### CFRP strips

The results for every corrosion level show increasing in load carrying capacity from 15.2 to 64.8%, 20.2–53.14%, and 38.2–58.8% for 11%, 26%, and 42% corrosion levels respectively. The CFRP strips would shred, delaminate as the load got closer to its maximum. Alongside these physical changes, there would also be a “crackling” sound that would indicate the CFRP’s collapse. When the cracks finally reached the slab’s compression zone, the concrete there was crushed, and the CFRP broke free and erupted off the slab.

#### NSM

For CFRP robs, load carrying capacity results show less values than CFRP strips and that’s because of the insertion of fiber ropes inside the concrete and their proximity to the steel reinforcement, which is exposed to corrosion and damage to the area surrounding the steel bars. The results show increasing in failure load from 15.2% to 38.76, 20.25–22.7%, and 38.2–31.7% for the mentioned corrosion levels. For the severe corrosion level, the result showed a decreasing in load capacity and that’s due to weakness of reinforcement steel and weakness of surrounding concrete for this corrosion level.

### Cracking development and failure mode

#### CFRP strips

The loading test may be conducted once all of the test apparatus had been examined. In the tension part of the pure bending section of the slab specimens, the first fracture emerged when the load was increased to 30–35 kN (at the 15% corrosion level). An increasing number of cracks appeared within the tensile zone as the load was raised. The breadth of the primary cracks grew along with the fissures’ complete appearance as the weight rose. Also, the cracks took less time than in the first case, as the first crack appeared at a load of 20–25 kN, and 10–15 kN for 28% and 42% corrosion levels respectively. This illustrates how much the reinforcing steel contributes to corrosion and how it isn’t as resistant to applied load as it was during the initial stages of corrosion.

#### NSM

When the load reached its maximum, CFRP robs wrinkled, delaminated, and ripped. A “crackling” sound would follow these physical changes, marking the CFRP’s disintegration. The fractures finally reached the slab’s compression zone, crushing the concrete and causing the CFRP to split and burst.

Figure (8) displays the crack profiles of slab specimens under ultimate loading. Each and every specimen has a flexible failure mode. The failure modes of every slab specimen

Table 4 Corroded steel bars details

Slab Symbol	Weight of steel bar before corrosion (gm)	Area of steel bar before corrosion (mm <sup>2</sup> )	Weight of steel bar after corrosion (gm)	Area of steel bar after corrosion (mm <sup>2</sup> )	Corrosion (%)
S 1	231	28	196	23.8	15.5
S 2	231	28	163	20.4	29.7
S 3	231	28	134	16.3	42.0



were significantly impacted by the amounts of corrosion on the reinforcing rebars.

**Midspan deflection response**

**CFRP Strips** The specimens strengthened with CFRP strips showed decreasing in midspan deflection from 33.5 to 16.2%, 73.1–44.57%, and 81.9–51.67% for 11%, 26%, and 42% corrosion levels respectively, and that decreasing due to steel bars weakness and their lack of resistance to

the applied loads. For CFRP strips, the midspan deflection show a gradually decreasing for every corrosion level until reached the minimum load failure at the strong corrosion level.

**NSM** The specimens reinforced with CFRP robs demonstrated a decrease in midspan deflection from 33.5 to 21.29%, 73.1–21.08%, and 81.9–37.29% for the mentioned corrosion levels. These midspan deflection values were due to the decreasing in the load carrying capacity of the models strengthening with this technique.

The load–midspan deflection curves for each slab are shown in Fig. (9). The inflection points generally divide the load–midspan deflection curves of S0 into three sections. During the early phase, the slab is in its elastic condition before the first fractures appear. The curve begins the second stage and its slope somewhat lowers after the first inflection point. The curve reaches the third stage following the second inflection point. Up to the maximal load, the slab specimens’ deflection increases quickly, and the curve modifies and becomes soft. The corrosion of the reinforcing rebars caused the corroded slab specimens to be less rigid than the control slab (S0).

Shown in Fig. (10), when the corrosion level increased, the binding behavior between the concrete and the reinforcing rebar degraded and the slab’s mechanism progressively changed from “slab action” to “arch action.” The load–midspan deflection curves of all the corroded slabs tended to be smoother as the corrosion level increased, and the yield platform of the reinforcing bars became less visible, making the inflection point less noticeable. Furthermore, as the corrosion level above 20%, the slab specimen’s final deflection dramatically reduced.

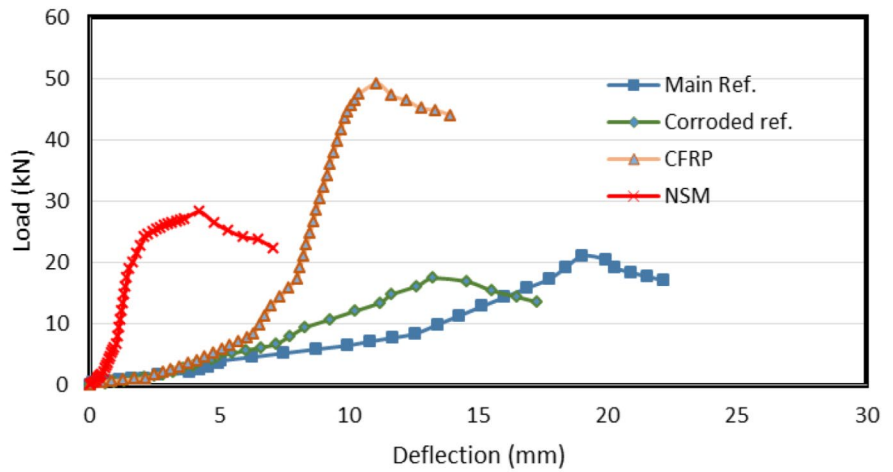
Upon corrosion of the longitudinal reinforcement, the carrying capacity of the concrete slabs, and the deflection decreasing for each corrosion percentage from the aforementioned, the load-deflection curves in Figs. (10) and (11) are evident. The benefits of adding CFRP reinforcement to the concrete slabs were evident: each slab’s bearing capacity rose to a greater extent than that of other slabs, indicating a weaker corrosion. This is because the corrosion process doesn’t have a significant impact on the iron. Additionally, the fiber-reinforced slabs’ bearing capacity dropped as the rate of corrosion rose. However, it continues to be stronger than the slab was prior to strengthening, demonstrating the robustness and high tensile resistance of the fibers utilized as well as the epoxy used.

Figure (12) depicts a comparison of two unique carbon fiber applications: carbon strips and NSM. Two ways were utilized to investigate the behavior of this fiber, and each



**Fig. 8** Failure Crack Modes for Tested slabs; a) and b) group 1, c) and (d) group 3, and e) group 2

**Fig. 9** Load–Deflection Curves for Group 1 (11% Corrosion Level)



**Fig. 10** Load-Deflection Curves for Group 2 (26% corrosion Level)

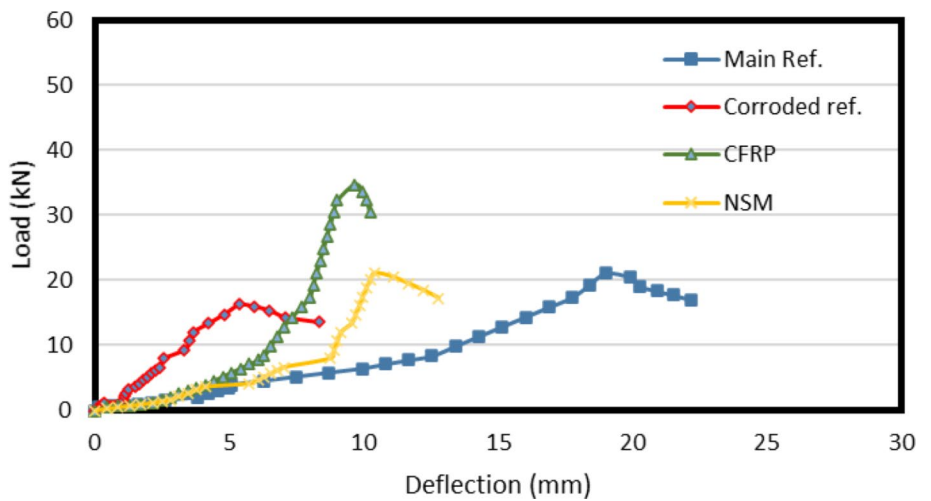
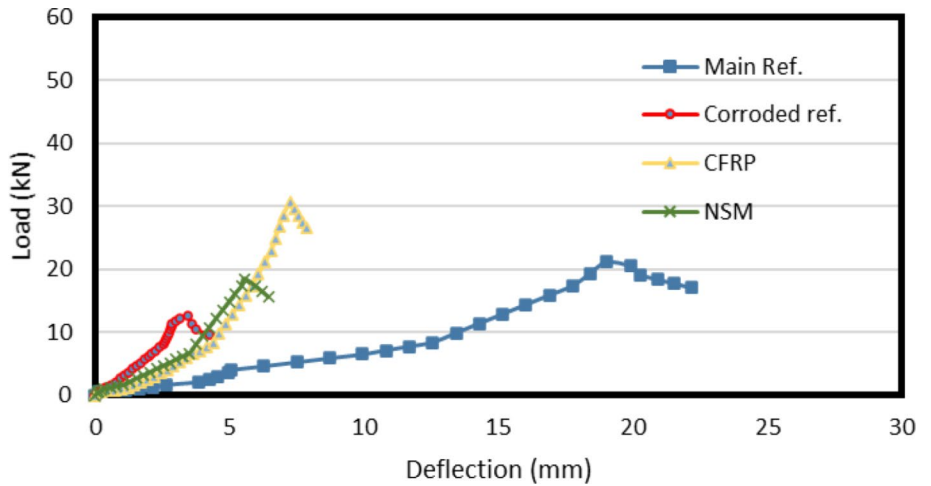


**Fig. 11** Load-Deflection Curves for Group 3 (42% Corrosion Level)



method’s endurance was determined. Figure (12) shows that carbon fiber strips surpass NSM in terms of endurance capacity. This is because the carbon strips were positioned at a wider distance from the damaged iron, yielding good outcomes, as compared to NSM, where the carbon fiber

ropes were placed closer to the iron, resulting in a drop in tensile strength. In terms of the drop caused by these two techniques, the deflection behavior was nearly comparable.



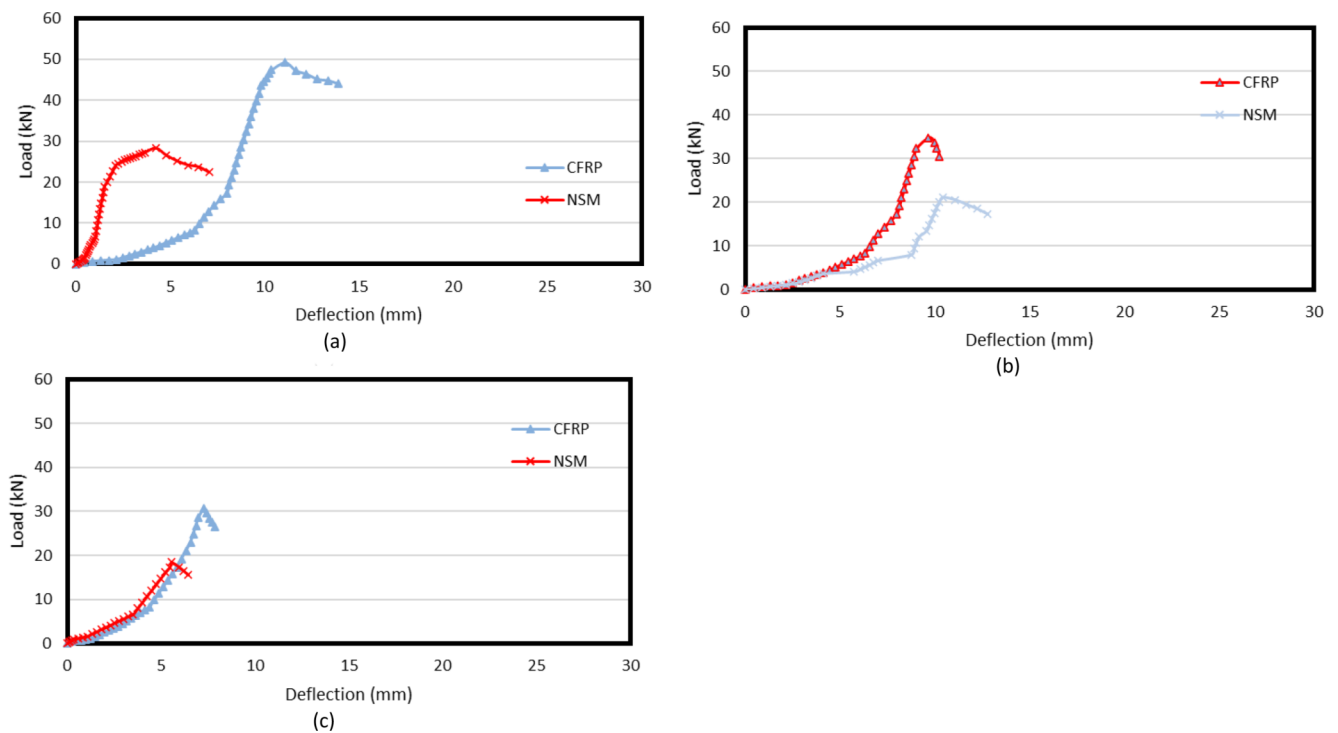


**Fig. 12** Comparison between Load –Deflection behavior for NSM and CFRP strips; **a)** Load –Deflection Curves for 11% corrosion Level, **b)** for 26%, and **c)** for 42%

### Conclusion

Accelerated corrosion was applied to the longitudinal reinforcing rebars of ten slab specimens that were manufactured. The slab specimens were reinforced with CFRP in two separate processes following the rebars’ deterioration. All specimen’s mechanical characteristics were measured. The experimental study’s outcome led to the following conclusions been reached.

1. Each slab specimen showed indications of flexural failure. The degree of corrosion on the reinforcing rebars had a significant impact on the failure mechanism of each slab specimen. Because the CFRP fractured and split off the slab specimen, all of them failed.
2. As the corrosion of the reinforcing rebars increased, the slab specimens’ rigidity somewhat reduced. But when the corrosion level exceeded 28%, the specimens’ final deflection dramatically dropped.
3. CFRP strips showed strong tensile strength at 15% corrosion, but CFRP grooves had low tensile strength at the same amount of corrosion.
4. As the corrosion level increases, the fibers’ bearing ability decreases, causing them to debond from the sample. For CFRP strips, the increases in bearing capacity were 15–65%, 20–53%, and 38–58% over 10, 17, and 24 days, respectively. Furthermore, for NSM, the findings

revealed an increase in bearing capacity from 15 to 38%, 20–23%, and a decrease in yielding strength for 40% corrosion from 38 to 31%. However, it was less than CFRP strips.

### References

1. Vaysburd AM, Emmons PH (2000) How to make today’s repairs durable for tomorrow—corrosion protection in concrete repair. *Constr Build Mater* 14:189–197
2. Mangat PS, Elgarf MS (1999) Flexural strength of concrete beams with corroding reinforcement. *ACI Struct J* 96:149–158
3. Wu Q, Yuan YS Experimental study on the deterioration of mechanical properties of corroded steel bars. *China Civ Eng J* 2008, 41, 42–47. (In Chinese)
4. Castel A, François R, Arliguie G (2000) Mechanical behaviour of corroded reinforced concrete beams—part 1: experimental study of corroded beams. *Mater Struct* 33:539–544
5. Castel A, François R, Arliguie G (2000) Mechanical behaviour of corroded reinforced concrete beams—part 2: bond and notch effects. *Mater Struct* 33:545–551
6. Coccia S, Imperatore S, Rinaldi Z (2016) Influence of corrosion on the bond strength of steel rebars in concrete. *Mater Struct* 49:537–551
7. Maheswaran J, Chellapandian M, Arunachalam N (2022) Retrofitting of severely damaged reinforced concrete members using fiber reinforced polymers: a comprehensive review. *Structures* 38:1257–1276
8. Van Cao V, Vo HB, Dinh LH, Van Doan D (2022) Experimental behavior of fire-exposed reinforced concrete slabs without and with FRP retrofitting. *J Build Eng* 51:104315

9. Wang WW (2007) FRP Strengthening of Concrete Structures; China Building Industry Press: Beijing, China, (In Chinese)
10. Soudki KA, Sherwood TG (2000) Behaviour of reinforced concrete beams strengthened with carbon fibre reinforced polymer laminates subjected to corrosion damage. *Can J Civ Eng* 27:1005–1010
11. Wang CY, Shih CC, Hong SC, Hwang WC (2004) Rehabilitation of cracked and corroded reinforced concrete beams with fiber-reinforced plastic patches. *J Compos Constr* 8:219–228
12. Kutarba MP (2004) Durability of Carbon Fiber Reinforced Polymer (CFRP) Strengthening Systems Used to Repair Corrosion Damage in Reinforced Concrete. Master's Thesis, University of Florida, Gainesville, FL, USA
13. Maaddawy TE, Soudki K (2005) Carbon-Fiber-Reinforced Polymer repair to extend service life of corroded reinforced concrete beams. *J Compos Constr* 9:187–194
14. Maaddawy TE, Soudki K, Topper T (2005) Computer-based mathematical model for performance prediction of corroded beams repaired with fiber reinforced polymers. *J Compos Constr* 9:227–235
15. Al-Saidy AH, Al-Harthy AS, Al-Jabri KS, Abdul-Halim M (2010) Al-Shidi, N.M. Structural performance of corroded RC beams repaired with CFRP sheets. *Compos Struct* 92:1931–1938
16. Wang XG Flexural Behavior of Corroded Reinforced Concrete Beams Strengthened with Carbon Fiber Composite Sheets., Thesis PD (2008) Tongji University, Shanghai, China, (In Chinese)
17. Hu RL, Su LW, Wang YY, Xie JH (2010) Experimental study on flexural capacity of corrosion-damaged RC beams repaired with different-layered. *Port Waterw Eng* 446:119–123 (In Chinese)
18. Davalos JF, Parish GC, Chen A, Ray I (2013) Effect of anchoring schemes for beams aged by accelerated corrosion and strengthened with carbon fibre-reinforced polymer. *Struct Infrastruct E* 9:229–241
19. Al-Saidy AH, Al-Jabri KS (2011) Effect of damaged concrete cover on the behavior of corroded concrete beams repaired with CFRP sheets. *Compos Struct* 93:1775–1786
20. Al-Saidy AH, Saadatmanesh H, El-Gamal S, Al-Jabri KS, Waris BM (2016) Structural behavior of corroded RC beams with/without stirrups repaired with CFRP sheets. *Mater Struct* 49:3733–3747
21. Badawi M, Soudki K (2010) CFRP repair of rc beams with shear-span and full-span corosions. *J Compos Constr* 14:323–335
22. Ray I, Parish GC, Davalos JF, Chen A (2010) Effect of concrete substrate repair methods for beams aged by accelerated corrosion and strengthened with CFRP. *J Aerosp Eng* 24:227–239
23. Yamamoto T, Hattori A, Miyagawa T (2003) Strengthening with CFRP sheet for RC flexural member deteriorated by reinforcing steel corrosion. In Proceedings of the 8th International Conference on Inspection Appraisal Repairs & Maintenance of Structures, Singapore, 18–19 December ; pp. 351–358
24. Kashi A, Ramezani-pour AA, Moodi F (2017) Durability evaluation of retrofitted corroded reinforced concrete columns with FRP sheets in marine environmental conditions. *Constr Build Mater* 151:520–533
25. Rose AL, Suguna K, Ragunath PN (2009) Strengthening of corrosion-damaged reinforced concrete beams with glass fiber reinforced polymer laminates. *J Comput Sci* 5:435–439
26. Deng ZC, Li JH, Lin HF (2009) Experimental study on flexural performance of corroded RC beams strengthened with afpr sheets. *Key Eng Mater*. 405–406, 343–349
27. Gotame M, Franklin CL, Blomfors M, Yang J, Lundgren K (2022) Finite element analyses of FRP-strengthened concrete beams with corroded reinforcement. *Eng Struct* 257:114007
28. Zheng A, Li S, Zhang D, Yan Y (2021) Shear strengthening of RC beams with corrosion-damaged stirrups using FRP grid-reinforced ECC matrix composites. *Compos Struct* 272:114229
29. Yang J, Haghani R, Blanksvärd T, Lundgren K (2021) Experimental study of FRP-strengthened concrete beams with corroded reinforcement. *Constr Build Mater* 301:124076
30. Li W, Huang Z, Huang Z, Yang X, Shi T, Xing F (2020) Shear behavior of RC beams with corroded stirrups strengthened using FRP laminates: Effect of the shear span-to-depth ratio. *J Compos Constr* 24:04020033–04020031
31. Chen C, Cai H, Cheng L (2021) Shear strengthening of corroded RC beams using UHPC-FRP composites. *J Bridge Eng.* 2,04020111-1-04020111-14
32. GB50367-2013; Code for Design of Strengthening Concrete Structure. Ministry of Housing and Urban-Rural Development of the People's Republic of China (MOHURD): Beijing, China (2013) ; p. 76. (In Chinese)

**Publisher's Note** Springer Nature remains neutral with regard to jurisdictional claims in published maps and institutional affiliations.

Springer Nature or its licensor (e.g. a society or other partner) holds exclusive rights to this article under a publishing agreement with the author(s) or other rightsholder(s); author self-archiving of the accepted manuscript version of this article is solely governed by the terms of such publishing agreement and applicable law.